

UDC 624.014

ALUMINUM DOME STRUCTURES' STABILITY STUDY

V.H. Tonkacheiev,

Candidate of Engineering Sciences, Associate Professor

S.I. Bilyk,

Doctor of Technical Sciences, Professor

H.M. Tonkacheiev,

Doctor of Technical Sciences, Professor

Kyiv National University of Construction and Architecture

DOI: 10.32347/2410-2547.2024.112.229-238

Abstract. The large spans dome structures made of aluminum alloys work is considered. The dome elements material choice is due to the lower weight compared to steel elements, the material corrosion resistance and the lower thermal expansion coefficient. A two-rod three-hinged model — the von Mises truss (MT) — was used as the research model. The normal stresses on relative deformations dependences graphs for a low-pitched truss with rod inclination angles of 80 and 85 degrees from the vertical for aluminum alloy 5083 with different tubular profiles thicknesses were obtained. The research was carried out in accordance with the provisions described in DSTU-NB EN 1999. An analytical expressions system was derived for determining the aluminum alloy elasticity modulus on strain diagrams. Analytical dependences describing the aluminum MT trusses' operation for all alloys with known mechanical and deformation properties have been obtained. The relative concentrated force in the truss's ridge node on the relative vertical deformations dependences graphs are plotted, taking into account the geometric and physical nonlinear material operation. The conducted research practical significance is that the obtained dependencies allow modeling the MT trusses with aluminum-based rods operation, taking into account various truss geometries. When modeling trusses, an inclined load and the presence of elastic supports in the ridge node were taken into account. Dependencies make it possible to predict the aluminum ribbed-ring domes stability loss, which are modeled by MT trusses.

Keywords: dome, stability, aluminum, alloy, tensile diagram, geometric nonlinearity, physical nonlinearity, von Mises truss.

The problem statement

Dome structures are one of the most efficient roof structures in terms of both material consumption and energy efficiency [1, 2].

Dome roofs are more often designed and built using steel structures. The steel structures advantages are high strength, low deformability, and dome elements joints manufacturability. The disadvantages are the dome's relatively high weight and its elements' high thermal expansion coefficient, which is important for roof structures exposed to direct sunlight. Steel elements have lower corrosion resistance compared to aluminum.

When designing an aluminum dome, you can create a truly unique rounded structure due to the material practicality. Aluminum has a long service life, light weight, relatively high mechanical strength and corrosion resistance. Together, all these properties create a unique product that will last for decades in any weather conditions.

Domes made of aluminum profiles do not contain harmful impurities and fully meet the environmental safety requirements.

One of the most important disadvantages is low temperature resistance, which consists in the material reduced strength when heated to certain temperatures (≥ 80 degrees), which for some alloys is, as a rule, lower than that of steel. This shortcoming must be taken into account during design, not only when calculating temperature resistance, but also when designing aluminum structures welded joints.

Another no less important aluminum alloys property is the material behavior under load. Ensuring the domes upper tiers' stability against concentrated loads remains a problematic issue.

Some aluminum alloys are also characterized by a non-linear relationship between stresses and strains. The linear deformation clearly defined area absence is usually taken into account by using physically nonlinear calculation models in the structures design.

The recent research and publications analysis

Many scientific works have been devoted to the aluminum and its alloys as materials properties study for building structures. Thus, in [3], the aluminum alloy samples stability and ultimate strength experimental research and study was carried out. In work [4], the aluminum alloy 6082-T6 columns stability under the axial compressive load action is investigated by finite element modeling. The work [5] is devoted to study the aluminum alloy I-beam columns' stability loss with torsional shape and the behavior after the stability loss. In [6], the thin-walled cross-section columns' experimental and numerical study of stability loss is considered. The irregularly shaped thin-walled aluminum alloy columns stability loss under axial compression experimental and numerical studies are given in [7]. An aluminum alloy T-shaped columns stability study is described in [8].

In works [9, 10], an aluminum alloy circular section tubular element stability under the axial loads action is studied. An aluminum alloy single corner fixed at one end stability loss is studied in the article [11]. The superplastic aluminum alloy 5083 mechanical behavior during the microforming process was investigated by the finite element method in [12]. The article [13] presents an equilibrium approach and a simplified energy method for the local and deformation extruded aluminum alloy corner columns stability loss. The article [14] describes an improved technique for constructing valid and effective aluminum alloy AMg2 (1520) deformation diagrams under uniaxial tension.

The regulatory document [15] recommends calculating aluminum structures using the material's elastic operation scheme, taking into account the constant elasticity modulus $E = 70,000$ MPa in the calculations. However, it does not exclude the performing calculations possibility taking into account physically non-linear work.

In DSTU-NB EN 1999-1-1:2010 [16], the nonlinear material operation is considered for three material operation models under load:

- bilinear model;
- trilinear model;
- continuous model.

The aluminum alloy ribbed-ring dome's work using the continuous model was considered.

The dome structures rods' stability was previously considered in works [17 - 21]. In works [17, 18], the ribbed-ring dome's generalized joints stability criterion was derived and investigated using the MT truss as a calculation model, under various initial load conditions and various initial dome geometric parameters, as well as the ridge node stiffness.

In work [19], the high domes operation and their asymmetric stability loss problem is considered.

The work [20] considered to the two-bar model stability loss with the ridge node bars elastic connection with hinged supports.

To study the aluminum ribbed-ring dome's stability under load, a two-bar three-hinged MT truss calculation model was used, which description is given in [17].

An aluminum MT truss structures caloptic behavior problem relates to the particularly critical structures' load-bearing capacity rapid loss general problem. This is important when taking into account the other force factors influence [22, 23], which change the metal's physical and mechanical characteristics, and there is a need to take into account the structure's nonlinear operation.

The problem formulation

Conduct a von-Mises truss nodal stability loss study, with the rods made of aluminum alloy 5083DT, under the concentrated load action in the ridge node using numerical simulation.

The main research material presentation.

The von Mises truss model as a model to study an aluminum ribbed-ring dome's buckling was chosen. The MT truss model which was used for numerical studies has the following geometrical and physical initial parameters (see Table 1).

Just as in work [21], the following notations were introduced:

- The relative vertical truss deformation is determined by the formula:

$$v[rel] = \frac{v_P}{a_0}, \quad (1)$$

where v_P – truss' ridge node vertical displacement; a_0 – an initial truss' half-span.

- The relative concentrated force in the ridge node determined by the formula:

$$P[rel] = \frac{P \cos \beta_p}{EA_{cal}}, \quad (2)$$

where P – concentrated force in the truss ridge node; β_p – the concentrated force inclination angle from the vertical; E – truss rod's material elasticity modulus; A_{cal} – the rods' calculated cross-sectional area.

Table 1

The MT three-hinged truss model parameters

Parameter name	Denotation	Value	Dimensionality
The initial rods inclination angles from the vertical	α_{0l}	80	degree
	α_{0l}	85	
1/2 of truss span	a_0	1	meter
Truss rod calculated cross-sectional area	A_{cal}	1	square meter
The ridge node's elastic supports stiffness (vertical and horizontal)	k_v	0	N·m
	k_f	0	
The Initial truss height at the rod angle from the vertical: 85 degrees / 80 degrees	f_0	$\frac{87.489}{176.327}$	millimeter

The system rods' relative deformations depend on the rods' inclination angles and on the concentrated load inclination angle at the truss ridge node [17]

$$\varepsilon_1 = 1 - \frac{(1 - \nu[rel] \tan \beta_p) \sin \alpha_{0l}}{\sin \alpha_{1l}}, \quad (3)$$

$$\varepsilon_2 = 1 - \frac{(1 + \nu[rel] \tan \beta_p) \sin \alpha_{0l}}{\sin \alpha_{2l}}, \quad (4)$$

where α_{0l} – the MT truss' rods initial angle.

$$\sin \alpha_{1l} = \frac{(1 - \nu[rel] \tan \beta_p)^2}{\sqrt{(1 - \nu[rel] \tan \beta_p)^2 + ((1/\tan \alpha_{0l}) - \nu[rel])^2}}, \quad (5)$$

$$\sin \alpha_{2l} = \frac{(1 + \nu[rel] \tan \beta_p)^2}{\sqrt{(1 + \nu[rel] \tan \beta_p)^2 + ((1/\tan \alpha_{0l}) - \nu[rel])^2}}, \quad (6)$$

According to Appendix E [16], to determine the normal stresses' dependence on relative strains ε , there are several approaches listed earlier. The approach described in paragraph E.2.2.1 was used to construct a smooth shape-continuing diagram. To do this, the diagram divided into 3 sections:

- elastic work;
- inelastic work;
- strain hardening.

Thus, the entire normal stresses dependence graph on relative deformations can be represented as an equations' system:

$$\sigma_i = \begin{cases} E\varepsilon_i & \text{at } 0 < \varepsilon_i \leq \varepsilon_p \\ f_e \left[0.2(\varepsilon_i/\varepsilon_e)^3 - (\varepsilon_i/\varepsilon_e)^2 + 1.85(\varepsilon_i/\varepsilon_e) - 0.2 \right] & \text{at } \varepsilon_p < \varepsilon_i \leq 1.5\overline{\varepsilon}_e \\ f_e \left[f_{\max}/f_e - 1.5((f_{\max}/f_e) - 1)(\overline{\varepsilon}_e/\varepsilon_i) \right] & \text{at } 1.5\overline{\varepsilon}_e < \varepsilon_i \leq \varepsilon_{\max} \end{cases}, \quad (7)$$

where i – the point number on the graph for which normal stresses are determined; $f_e = f_0$ - conditional elastic limit; $\overline{\varepsilon}_e = \frac{f_e}{E}$; $\varepsilon_p = 0.5\overline{\varepsilon}_e$ - strain corresponding to stress f_e ; $f_{\max} = f_u$ — tensile force at the

curve's top; $\varepsilon_{\max} = 0,5\varepsilon_u$ — strain corresponding to stress f_{\max} ; $\varepsilon_u = 0.30 - 0.22(f_e/400)$ — the ultimate deformation nominal value at $f_e < 400 \text{ N/mm}^2$; $E = 70000 \text{ N/mm}^2$ - aluminum elastic modulus.

Section $0 < \varepsilon_i \leq \varepsilon_p$ is characterized by a linear relationship between stresses and strains, corresponding to Hooke's law.

Section $\varepsilon_p < \varepsilon \leq 1.5\bar{\varepsilon}_e$, which is an inelastic work section, is characterized by a nonlinear relationship between stresses and strains, described by a third-degree polynomial

Section $1.5\bar{\varepsilon}_e < \varepsilon \leq \varepsilon_{\max}$ - deformation strengthening section for the aluminum alloy under study.

For the study, it was decided to use aluminum alloy 5083 DT, corresponding to the extruded pipe profile. Strength indicators for such alloys are shown in Table 2.

Table 2

Strength and relative deformation indicators of alloy 5083 DT

EN-AW alloy	Product shape	Thickness, mm	f_0 , N/mm ²	f_u , N/mm ²	$\bar{\varepsilon}_e$	ε_p	ε_u
5083	DT	$t < 10$	200	280	2.857e-3	1.429e-3	0.190
		$t < 5$	235	300	3.357e-3	1.679e-3	0.171

The MT truss stability study was carried out by modeling the truss' operation according to a deformed scheme. The model chosen was a symmetrical MT truss without elastic supports in the ridge node, which parameters were described earlier (see Table 1).

First, in iteration, the each truss rod relative deformations were determined using formulas (3) and (4). Then, for each relative strain value, a suitable region on the tensile diagram was determined, and then, according to the system of formulas (7), the normal stress value was determined for the corresponding point on the diagram. Then the relationship graph between stresses and relative deformations was plotted for each truss rod (Fig. 1, 2).

To determine the elastic modulus for each point on the dependence diagram (see Fig. 1,2), tangent value of tangent's angle was determined:

$$E_i = \tan \varphi_i = \frac{d\sigma_i}{d\varepsilon_i}, \quad (8)$$

where i – point number on the graphs (see Fig. 1, 2).

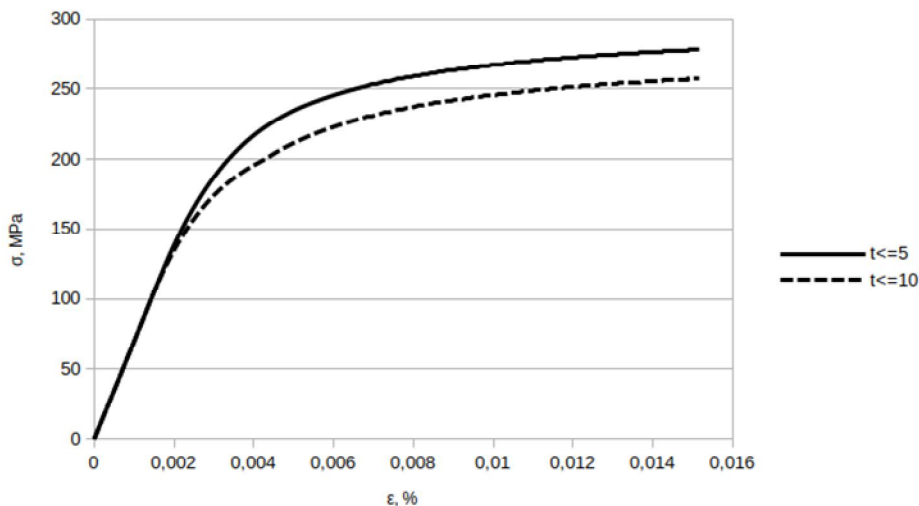


Fig. 1. Aluminum alloy 5083DT tensile diagram for the MT truss model at 80 degrees rods' inclination angle from the vertical: σ – normal stresses in the rods, MPa; ε – relative truss rods' deformation during compression, %; t – aluminum profile wall thickness, mm

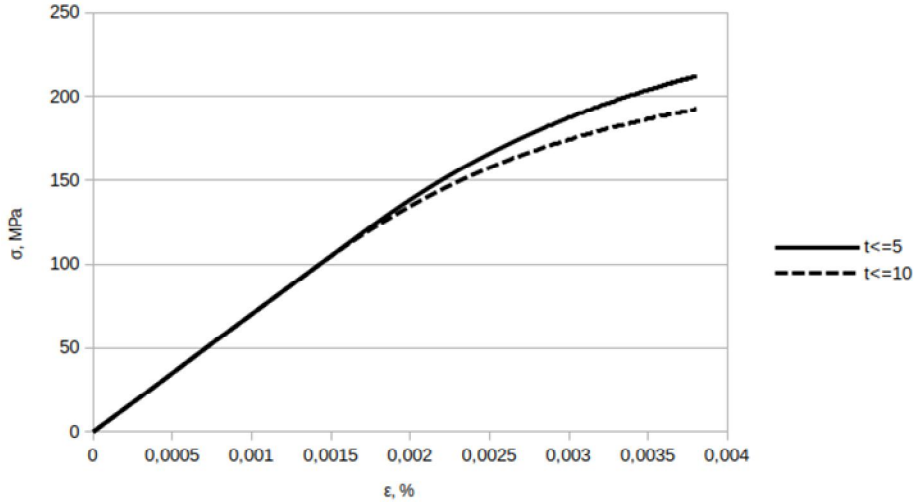


Fig. 2. Aluminum alloy 5083DT tensile diagram for the MT truss model at 85 degrees rods' inclination angle from the vertical:
 σ – normal stresses in the rods, MPa; ε – relative truss rods' deformation during compression, %;
 t – aluminum profile wall thickness, mm

According to expression (8), for each tensile diagram section, the normal stresses dependence derivative on relative deformations can be presented as equations system:

$$E_i = \frac{d\sigma_i}{d\varepsilon_i} = \begin{cases} E & \text{at } 0 < \varepsilon_i \leq \varepsilon_p \\ \frac{f_e}{20\varepsilon_e^2} (12\varepsilon_i^2 - 40\varepsilon_e \varepsilon_i + 37\varepsilon_e^2) & \text{at } \varepsilon_p < \varepsilon_i \leq 1.5\varepsilon_e \\ (3\varepsilon_e (f_{\max} - f_e)) / 2\varepsilon_i^2 & \text{at } 1.5\varepsilon_e < \varepsilon_i \leq \varepsilon_{\max} \end{cases}, \quad (9)$$

where i – point number on the graphs (see Fig. 1, 2).

After determining the elastic modulus values for each point on the tensile diagram, according to the system of equations (9), the truss ridge node relative concentrated force value was determined according to the formulas given in [17].

Taking into account the previously introduced notation (1), the expression will look like:

$$\frac{P \cos \beta_p}{EA_{cal}} - \frac{v_p k_v}{EA_{cal}} = \frac{1}{\sqrt{\frac{(1 - v[rel] \tan \beta_p)^2}{((1/\tan \alpha_{0l}) - v[rel])^2} + 1}} + \frac{1}{\sqrt{\frac{(1 + v[rel] \tan \beta_p)^2}{((1/\tan \alpha_{0l}) - v[rel])^2} + 1}} - 2 \sin \alpha_{0l}, \quad (10)$$

where P – concentrated force in the truss ridge node; β_p – the concentrated force inclination angle from the vertical; α_{0l} – the truss rods' initial inclination angle; E – rod's material elasticity modulus; A_{cal} – truss rods' calculated cross-sectional area; v_p – the truss ridge node's vertical displacement; k_v – the truss vertical supports' rigidity; $v[rel]$ – the truss' relative deformation according to (1).

For the further transformations convenience, the expression's parts (8) are designated as A and B for the expression part on the left and right, respectively, thus obtaining:

$$A = \frac{P_i \cos \beta_p}{E_i A_{cal}} - \frac{v_{pi} k_v}{E_i A_{cal}}, \quad (11)$$

$$B = \frac{1}{\sqrt{\frac{(1 - v[rel] \tan \beta_p)^2}{((1/\tan \alpha_{0l}) - v[rel])^2} + 1}} + \frac{1}{\sqrt{\frac{(1 + v[rel] \tan \beta_p)^2}{((1/\tan \alpha_{0l}) - v[rel])^2} + 1}} - 2 \sin \alpha_{0l}, \quad (12)$$

where i – point number on the graphs (see Fig. 1, 2).

If we substitute the elastic modulus value into expression (11) according to system (9), then we will have the following expressions' system:

$$A_i = \begin{cases} \frac{P_i \cos \beta_p}{EA_{cal}} - \frac{v_{pi} k_v}{EA_{cal}} & \text{at } 0 < \varepsilon_i \leq \varepsilon_p \\ \frac{20 P_i \bar{\varepsilon}_e^3 \cos \beta_p}{f_e (12 \bar{\varepsilon}_i^2 - 40 \bar{\varepsilon}_e \bar{\varepsilon}_i + 37 \bar{\varepsilon}_e^2) A_{cal}} - \frac{20 \bar{\varepsilon}_e^3 v_{pi} k_v}{f_e (12 \bar{\varepsilon}_i^2 - 40 \bar{\varepsilon}_e \bar{\varepsilon}_i + 37 \bar{\varepsilon}_e^2) A_{cal}} & \text{at } \varepsilon_p < \varepsilon_i \leq 1.5 \bar{\varepsilon}_e \\ \frac{2 P_i \bar{\varepsilon}_i^2 \cos \beta_p}{3 \bar{\varepsilon}_e (f_{max} - f_e) A_{cal}} - \frac{2 \bar{\varepsilon}_i^2 v_{pi} k_v}{3 \bar{\varepsilon}_e (f_{max} - f_e) A_{cal}} & \text{at } 1.5 \bar{\varepsilon}_e < \varepsilon_i \leq \varepsilon_{max} \end{cases} \quad (13)$$

Thus, by combining the expressions' system (13) and expression (12) in the expression form A=B, we can determine the force Pi value for each point i on the diagrams.

The numerical simulation results are presented at graphs (Fig. 3, 4).

As can be seen at the graphs (see Fig. 3, 4), at first the truss' deformation occurs slowly according to a nonlinear dependence, and after the truss loses stability, more rapid deformation occurs because of the ridge node snap-through collapse. At the same time, interestingly, for a truss with the 80 degrees rods initial inclination angle, the stability loss occurred in the deformation strengthening zone on the graph (see Fig. 1), which is characterized by deformations $1.5 \bar{\varepsilon}_e < \varepsilon \leq \varepsilon_{max}$.

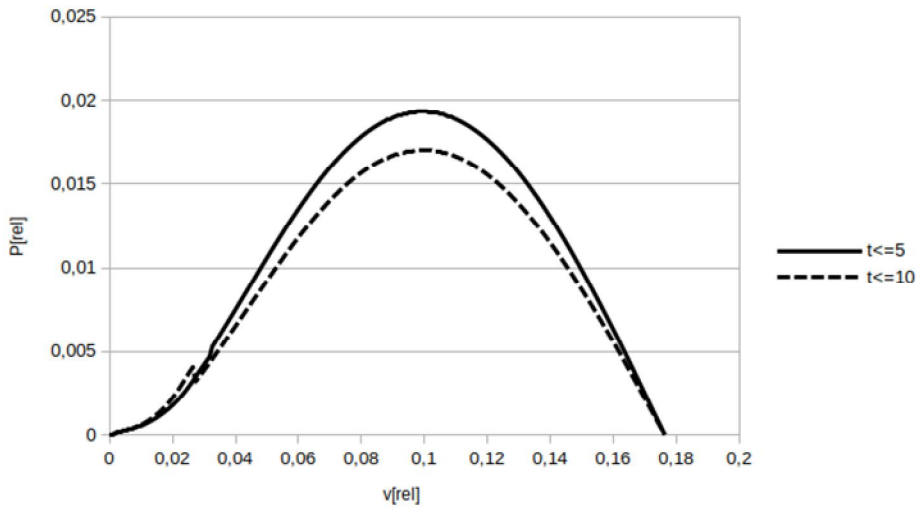


Fig. 3. The relative concentrated force at the MT truss ridge node $P[rel]$ dependence graph on the relative vertical deformations $v[rel]$ for aluminum alloy 5083DT at the 80 degrees rods' inclination angle from vertical of : t - the wall thickness of aluminum profile, mm

For a truss with the 85 degrees rods initial inclination angle from the vertical, the stability loss occurred somewhat earlier, compared to a truss with the 80 degrees inclination angle. The truss stability loss occurred in the inelastic deformation zone on the graph (see Fig. 2). which is characterized by deformations $\varepsilon_p < \varepsilon \leq 1.5 \bar{\varepsilon}_e$. It can also be noted that the truss deformation in the aluminum elastic work zone occurs more slowly than that observed in the inelastic operation and strain hardening zones.

Jumps on the graphs (see Fig. 3, 4) are associated with changes in the derivatives values determined from expressions (9) and (13). The jump on the graph (see Fig. 3) is associated with a change from section 2 ($\varepsilon_p < \varepsilon \leq 1.5 \bar{\varepsilon}_e$) to section 3 ($1.5 \bar{\varepsilon}_e < \varepsilon \leq \varepsilon_{max}$) on the diagram (see Fig. 1). The jump on the

graph (see Fig. 4) is associated with a change from section 1 ($0 < \varepsilon \leq \varepsilon_p$) to section 2 ($\varepsilon_p < \varepsilon \leq 1.5\overline{\varepsilon}_e$) on the diagram (see Fig. 2).

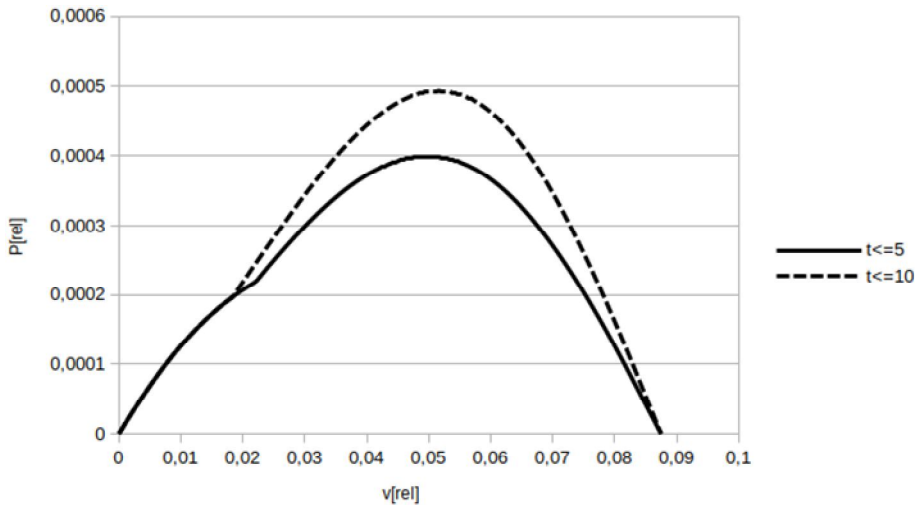


Fig. 4. The relative concentrated force at the MT truss ridge node $P[rel]$ dependence graph on the relative vertical deformations $v[rel]$ for aluminum alloy 5083DT at the 85 degrees rods' inclination angle from vertical of : t - the wall thickness of aluminum profile, mm

To obtain the MT truss relative vertical force dependences graphs on the relative vertical deformations without jumps, it is necessary, instead of using the values obtained from expressions (9) or (13), to search for approximated dependences for the graphs (Fig. 1, 2). In this case, special attention should be paid to places on the approximated diagrams where the dependence graph goes from rising to declining, which will give zero and negative elastic modulus values.

Conclusions

1. The ribbed-ring dome deformations made of aluminum alloy 5083DT numerical modeling with the MT truss model, and loaded at the ridge unit with a vertical concentrated load was performed. The modeling takes into account the three-hinged truss model geometric nonlinearity and the truss rods material physical nonlinearity.
2. According to the Appendix E [16] provisions, the normal stresses dependences graphs in the MT truss rods on these rods' relative deformations arising during truss deformation were obtained.
3. The expressions systems (9) and (13) are derived that allow the elastic modulus to be determined for the MT truss, taking into account the aluminum materials operation physically nonlinear model, not only for the materials given in [16], but also for any aluminum-based materials, for which their strength-deformation characteristics have been determined by testing, as is done in Table 2.
4. The relative concentrated load in the the truss ridge node dependences graphs on the ridge node relative vertical displacements were obtained.
5. The MT trusses deformation analysis, which rods are made of aluminum-based materials, showed nonlinear relationships between the truss vertical deformations and the concentrated nodal load; the deformation nature in the elastic deformations zone is slower than in the elastic deformations and deformation strengthening zones.
6. The research practical significance is that the obtained dependencies (9), (12), (13) make it possible to simulate any MT trusses with rods made of aluminum-based materials, taking into account any truss geometry, various initial parameters, such as an inclined load presence and an elastic supports presence in the ridge node. This allows us to predict the ribbed-ring domes stability loss modeled using MT trusses.

REFERENCES

1. *Bilyk S. I.* Ratsionalna forma heometrychnoi skhemy ramnoho karkasu z karnyznymy pokhlylmy elementamy navkolo funktsionalnogo ob'iemu (Optimal form of the geometrical circuitry of the frame carcass with incline elements around functional cubature) // Applied geometry and engineering graphics: Collection of scientific papers/ KNUBA. –K., 2004. – V. 74. – P. 228–235. [in Ukrainian].
2. Problemy konstruiuvannya rebrysto-kiltsevykh kupoliv (Problems of designing ribbed-ring domes) / *Bilyk S.I., Tonkacheev V.H.* // System technologies. Scientific collection – D.: Ministry of Education of Ukraine. – 2018 – No. 5 (118). – pp. 166-170. Electronic resource: http://st.nmetau.edu.ua/journals/118/20_a_ua.166-170.pdf [in Ukrainian]
3. *Odd S., Hopperstad, Magnus Langseth, Tore Tryland.* Ultimate strength of aluminium alloy outstands in compression: experiments and simplified analysis, *Thin-Walled Structures*, Volume 34, Issue 4, 1999, Pages 279-294, [https://doi.org/10.1016/S0263-8231\(99\)00013-0](https://doi.org/10.1016/S0263-8231(99)00013-0).
4. *Wang Y, Lin S, Feng F, Zhai X, Qian H.* Numerical simulation of aluminum alloy 6082-T6 columns failing by overall buckling. *Advances in Structural Engineering*. 2016;19(10):1547-1574. doi:10.1177/1369433216643899.
5. *CzeslawSzymczak, Marcin Kujawa.* Torsional buckling and post-buckling of columns made of aluminium alloy, *Applied Mathematical Modelling*, Volume 60, 2018, Pages 711-720, <https://doi.org/10.1016/j.apm.2018.03.040>.
6. *Mei Liu, Lulu Zhang, Peijun Wang, Yicun Chang.* Buckling behaviors of section aluminum alloy columns under axial compression, *Engineering Structures*, Volume 95, 2015, Pages 127-137, <https://doi.org/10.1016/j.engstruct.2015.03.064>.
7. *Yicun Chang, Mei Liu, Peijun Wang, Xiulin Li,* Behaviors and design method for distortional buckling of thin-walled irregular-shaped aluminum alloy struts under axial compression, *Engineering Structures*, Volume 153, 2017, Pages 118-135, <https://doi.org/10.1016/j.engstruct.2017.10.014>.
8. *Gao, Y. T., & Hu, X.* (2011). Material Test on Aluminum Alloy Round Pipe for Building Structure. In *Advanced Materials Research (Vols. 194–196, pp. 981–984)*. Trans Tech Publications, Ltd. <https://doi.org/10.4028/www.scientific.net/amr.194-196.981>
9. *Lin Yuan, Qilin Zhang.* Buckling behavior and design of concentrically loaded T-section aluminum alloy columns, *Engineering Structures*, Volume 260, 2022, 114221, <https://doi.org/10.1016/j.engstruct.2022.114221>.
10. *Gao, Y. T., He, T., & Fu, P. B.* (2011). Stability Test on Aluminum Alloy Round Pipe for Structure. In *Advanced Materials Research (Vols. 368–373, pp. 253–257)*. Trans Tech Publications, Ltd. <https://doi.org/10.4028/www.scientific.net/amr.368-373.253>
11. *Zhaoyu Xu, Genshu Tong, Lei Zhang, Yong Guo.* Testing, modelling and design of aluminium alloy single-angle members connected by one leg under eccentric compression, *Thin-Walled Structures*, Volume 184, 2023, 110474, <https://doi.org/10.1016/j.tws.2022.110474>.
12. *Abu Mowazem HOSSAIN, Sung-Tae HONG, Kyu-Yeol PARK, Young-Sang NA.* Microforming of superplastic 5083 aluminum alloy, *Transactions of Nonferrous Metals Society of China*, Volume 22, Supplement 3, 2012, Pages s656-s660, [https://doi.org/10.1016/S1003-6326\(12\)61781-6](https://doi.org/10.1016/S1003-6326(12)61781-6).
13. *Zhaoyu Xu, Genshu Tong, Lei Zhang, Yong Guo.* Local and distortional buckling of extruded aluminium alloy lipped angle columns, *Structures*, Volume 34, 2021, Pages 3894-3905, <https://doi.org/10.1016/j.istruc.2021.10.014>.
14. *Pham D.K., Halimon A.P.* Povrezhdennost' i e'fektivnaya diagramma deformirovaniya alyuminiyevogo splava AMG2 (Damage and effective deformation diagram of AMG2 aluminum alloy) // *Bulletin of NTUU "KPI". Series of mechanical engineering - Kyiv: NTUU KPI, 2014. - No. 3 (72). - P. 145-151. Electronic resource: https://ela.kpi.ua/bitstream/123456789/15897/1/22.pdf* [in Ukrainian]
15. DBNV.2.6-165:2011 Konstruktsii budynkiv i sporud. Aluminievi konstruktsii. Osnovni polozhennia (DBN V.2.6-165:2011 Structures of buildings and structures. Aluminum structures. Basic provisions). Electronic resource: https://e-construction.gov.ua/laws_detail/3075006468928308288?doc_type=2 [in Ukrainian].
16. DSTU-NB EN 1999-1-1:2010 Yevrokod 9. Proektuvannia aliuminiyevykh konstruktsii. Chastyna 1-1. Zahalni pravyla dlia konstruktsii (DSTU-N B EN 1999-1-1:2010 Eurocode 9. Design of aluminum structures. Part 1-1. General design rules (EN 1999-1-1:2007, IDT). Electronic resource: <https://uscc.ua/dstu-n-b-en-1999-1-12010-vrokod-9-proektuvannya-alyuminiyevykh-konstruktsiy-chastyna-1-1-zagalni-pravila-dlya-konstruktsiy-en-1999-1-12007-idt> [in Ukrainian]
17. *Bilyk S.I., Tonkacheiev V.H.* The influence of direction of the nodal load on stability of the von Mises truss with elastic supports on the example of ribbed domes with rings of steel// *Construction, materials science, mechanical engineering. Section: Innovative lifecycle technology of housing and civil, industrial and transportation purposes – Dnepr: PGASA, 2015. – Issue No 85. – P. 44-49. http://smm.pgasa.dp.ua/article/view/67272*
18. *Bilyk S. I., Tonkacheiev V. H.* Chyslovi doslidzhennia vplyvu na stiikest ferm Mizesa hrebenevoi pruzhnoi opory pry pokhlylomu navantazheni (Mises trusses stability numerical studies with ridge elastic support under inclined loading) / *Bulletin of the Odessa State Academy of Construction and Architecture. Issue No. 61, "Zovnishreklamservice" LLC, ODABA, O.: 2016. - pp. 35-39, [in Ukrainian].*
19. *Bilyk S.I., Tonkacheiev H.M., Bilyk A.S., Tonkacheiev V.H.* Tall von-Mises trusses' skew-symmetric deformation // *Strength of Materials and Theory of Structures. - Kyiv: KNUBA, 2020. - Issue 105. - P.114 - 126. DOI: 10.32347/2410-2547.2020.105.114-126.*
20. *Bilyk S.I.* Stability of two-rod trusses taking into account the elastic stiffness of the ridge node // *Collection of scientific works of the Ukrainian Institute of Steel Structures named after V.M. Shimanovsky. – 2015. – Issue No 16. – P. 13-21. [in Ukrainian].*
21. *Sergiy Bilyk, Vitaliy Tonkacheiev.* Determining sloped-load limits inside von Mises truss with elastic support. *Materiali in tehnologije., Ljubljana, Slovenija* 52 (2018), 105-109, doi:10.17222/mit.2016.083.
22. *Shugaylo O-r P., Bilyk S.I.* Research of the stress-strain state for steel supportstructures of nuclear power plant components under seismic loads. *Nuclear and Radiation Safety.* 2022. № 3(95). C. 15-26. [https://doi.org/10.32918/nrs.2022.3\(95\).02](https://doi.org/10.32918/nrs.2022.3(95).02).
23. *Shugaylo O.-r, &Bilyk, S.* (2023). Rozvytok metodiv otsinky bezpeky stalevykh opornykh konstruktsii obladnannia i truboprovodiv enerhoblokov atomnykh stantsii za seismichnykh navantazhen (Development of Safety Assessment Methods for Steel Support Structures of Nuclear Power Plant Equipment and Piping under Seismic Loads) / *Nuclear and Radiation Safety, (1(97), 20-29. https://doi.org/10.32918/nrs.2023.1(97).03. [inUkrainian]*

Tonkacheiev V.H., Bilyk S.I., Tonkacheiev H.M.

ALUMINUM DOME STRUCTURES' STABILITY STUDY

The large spans dome structures made of aluminum alloys work is considered. The dome elements material choice is due to the lower weight compared to steel elements, the material corrosion resistance and the lower thermal expansion coefficient. An existing scientific research analysis related to the structures made of aluminum or aluminum alloys stability loss problem was carried out. A two-rod three-hinged model — the von Mises truss (MT) — was used as the research model. The normal stresses on relative deformations dependences graphs for a low-pitched truss with rod inclination angles of 80 and 85 degrees from the vertical for aluminum alloy 5083 with different tubular profiles thicknesses were obtained. The research was carried out in accordance with the provisions described in DSTU-NB EN 1999. An analytical expressions system was derived for determining the aluminum alloy elasticity modulus on strain diagrams. Analytical dependences describing the aluminum MT trusses' operation for all alloys with known mechanical and deformation properties have been obtained. The relative concentrated force in the truss's ridge node on the relative vertical deformations dependences graphs are plotted, taking into account the geometric and physical nonlinear material operation. The conducted research practical significance is that the obtained dependencies allow modeling the MT trusses with aluminum-based rods operation, taking into account various truss geometries. When modeling trusses, an inclined load and the presence of elastic supports in the ridge node were taken into account. Dependencies make it possible to predict the aluminum ribbed-ring domes stability loss, which are modeled by MT trusses.

Keywords: dome, stability, aluminum, alloy, tensile diagram, geometric nonlinearity, physical nonlinearity, von Mises truss.

Тонкачев В.Г., Білик С.І., Тонкачев Г.М.

ДОСЛІДЖЕННЯ СТІЙКОСТІ КУПОЛЬНИХ КОНСТРУКЦІЙ З АЛЮМІНІЮ

Розглядаються робота купольних конструкцій великих прольотів зі сплавів алюмінію. Вибір матеріалу елементів куполу обумовлений меншою вагою у порівнянні зі сталевими елементами, корозійною стійкістю матеріалу, меншим коефіцієнтом теплового розширення. Проведено аналіз існуючих наукових досліджень пов'язаних із проблемою втрати стійкості конструкцій, що виготовлено з алюмінію або алюмінієвих сплавів. Досліджена проблема втрати стійкості конструкцій ребристо-кільцевих куполів виконаних з алюмінієвих сплавів. У якості моделі дослідження використано двострижневу тришарнірну модель — ферму фон-Мізеса (ФМ). Отримано графіки залежностей нормальних напружень від відносних деформацій для положистої ферми з кутами нахилу стрижнів — 80 та 85 градусів від вертикалі для сплаву алюмінію 5083, різних за товщиною трубчастих профілів. Дослідження виконувались відповідно до положень, що описані в ДСТУ-Н Б EN 1999. Виведено систему аналітичних виразів для визначення модуля пружності алюмінієвого сплаву на діаграмах розтягу. Отримано аналітичні залежності, що описують роботу ферм ФМ з алюмінію для всіх сплавів, для яких відомі механічні та деформаційні властивості. Побудовано графіки залежностей відносною зосередженої сили в гребеневому вузлу ферми від відносних вертикальних деформацій з урахуванням геометричної та фізичної нелінійної роботи матеріалу. Практична значимість проведених досліджень полягає в тому, що отримані залежності дозволяють моделювати роботу ферм ФМ зі стрижнями на основі алюмінію із урахуванням різноманітної геометрії ферми. При моделюванні ферм враховується наявність похилого навантаження та присутність пружних опор в гребеневому вузлу. Залежності дозволяють прогнозувати втрату стійкості алюмінієвих ребристо-кільцевих куполів, які моделюються фермами ФМ.

Ключові слова: купол, стійкість, алюміній, сплав, діаграма розтягу, геометрична нелінійність, фізична нелінійність, ферма фон-Мізеса.

УДК 624.014

Тонкачев В.Г., Білик С.І., Тонкачев Г.М. Дослідження стійкості купольних конструкцій з алюмінію // Опір матеріалів і теорія споруд: наук.-тех. збірник – К.: КНУБА, 2024. – Вип. 112. – С. 229-238. – Англ.

Досліджено стійкість положистих ребристо-кільцевих куполів виконаних з алюмінієвих сплавів змодельованих за допомогою ферми фон Мізеса.

Іл. 4. Бібліогр. 23 назв.

UDC 624.014

Tonkacheiev V.H., Bilyk S.I., Tonkacheiev H.M. Aluminum dome structures' stability study // Strength of Materials and Theory of Structures: Scientific-and-technical collected articles. – K.: KNUBA, 2024. – Issue 112. – P. 229-238.

The low-pitched ring-ribbed domes stability made of aluminum alloys modeled via von Mises trusses is considered.

Fig. 4. Ref. 23.

Автор (науковий ступінь, вчене звання, посада): кандидат технічних наук, доцент кафедри металевих та дерев'яних конструкцій КНУБА ТОНКАЧЕВ Віталій Геннадійович

Адреса робоча: 03680 Україна, м. Київ, проспект Повітряних сил, 31, Київський національний університет будівництва і архітектури.

Адреса домашня: 08136 Україна, с. Крюківщина, вул. Дружби 6, кв. 19, Тонкачеву Віталію Геннадійовичу

Мобільний тел.: +38(063) 322-40-50

Домашній тел.: +38(044) 545-50-49

E-mail: tonkacheiev.vg@knuba.edu.ua

ORCID ID: <https://orcid.org/0000-0002-1010-8440>

Автор (науковий ступінь, вчене звання, посада): доктор технічних наук професор, професор кафедри металевих та дерев'яних конструкцій, завідувач кафедри металевих та дерев'яних конструкцій КНУБА БІЛІК Сергій Іванович.

Адреса робоча: 03680 Україна, м. Київ, проспект Повітряних сил, 31, Київський національний університет будівництва і архітектури.

Адреса домашня: 02068 Україна, м. Київ, вул. Драгоманова 23, кв. 03, Білику Сергію Івановичу.

Робочий тел.: +38(044) 241-55-56

Мобільний тел.: +38(067) 098-044-82 88

Домашній тел.: +38(098) 044-82-88

E-mail: vartist@ukr.net

ORCID ID: <https://orcid.org/0000-0001-8783-5892>

Автор (науковий ступінь, вчене звання, посада): доктор технічних наук, професор кафедри будівельних технологій, завідувач кафедри будівельних технологій КНУБА ТОНКАЧЕСВ Геннадій Миколайович

Адреса робоча: 03680 Україна, м. Київ, проспект Повітряних сил, 31, Київський національний університет будівництва і архітектури.

Адреса домашня: 08136 Україна, с. Крюківщина, вул. Дружби 6, кв. 19, Тонкачєєву Геннадію Миколайовичу

Мобільний тел.: +38(050) 922-84-13

E-mail: tonkacheiev.gm@knuba.edu.ua

ORCID ID: <https://orcid.org/0000-0002-6589-8822>